

**THEORETICAL AND EXPERIMENTAL STUDIES OF DYNAMIC BEHAVIOR OF
UNDERGROUND CYLINDRICAL STRUCTURES UNDER THE INFLUENCE OF SEISMIC
EXPLOSION WAVES**

¹Teshaev Muhsin Khudoyberdiyevich, ²Safarov Ismoil Ibrohimovich, , ³Rakhmonov Bakhtiyor Sobirovich,
⁴Sagdiyev Hamidulla Sagdiyevich

¹ Professor of Department of Higher Mathematics, Bukhara engineering-technological institute, 15, Murtazayev str., Bukhara city, Uzbekistan,

² Head of Department of Higher Mathematics, Tashkent Institute of Chemistry and Technology, 32, Navoi str., Tashkent city, Uzbekistan.

³ Department of "Mechanics", Urgench State University, 14, Kh. Alimdjan str., Urgench city, Uzbekistan,

⁴ Director of Research Institute of Mechanics and Earthquake Resistance, 3, Do'rmon yo'li str., Tshkent city, Uzbekistan.

Abstract. In this article an experimental study (for large-scale underground explosions) and theoretical studies of the behavior of thin-walled cylindrical pipeline structures in soil environments under the influence of seismic blast waves is devoted. It is known that, currently in the world, in particular in Uzbekistan, seismic shocks are observed, as well as various natural and man-made disasters. For the first time, a description is given of the statement of the problem of the effect of seismic blast waves on a cylindrical structure. Methods for conducting large-scale field experiments to determine the dynamic behavior of thin-walled cylindrical structures, located in the soil environment, are also described.

The main goal of the work is to study the dynamic behavior of underground cylindrical structures in steel shells located in soil environments under the influence of seismic blast waves experimentally, and their theoretical justification. And also, the study of the kinematic parameters of the soil and the dynamic stress-strain state of cylindrical structures theoretically and experimentally. For the theoretical solution of problems, algorithms are constructed and programs are compiled using the methods and equations of the theory of elasticity and plasticity, as well as equations of the linear theory of shells (according to the Kirchhoff-Love hypothesis).

To maximize the description of the physical nature of the interaction during the experiments, along with seism metric observations, tens metric observations were simultaneously carried out.

Records of longitudinal, transverse and vertical movements of the cylindrical structure (pipe) at the points are obtained. The results of experimental studies coincide with theoretical results with a difference of up to

40%. Also, in experimental studies of cylindrical structures, results were obtained that take into account edge effects.

Keywords: cylindrical structure, underground explosion, seismic blast waves, soil environment, dynamic behavior.

1. Introduction

Seismic effects of blasting on various objects was investigated in the works of M.A. Sadovsky [1,2], G.M. Lyakhov [3,4], V.V. Adushkin [5,6], B.N. Kutuzov [7], S.V. Medvedev [8], B.V. Equist [9], A.P. Gospodarikov [10] and others. To study the process of the effect of seismic blast waves on a structure, mainly experimental (or analytical) methods were used. Approximate solutions to the problem of a plane one-dimensional explosive wave were G.M. Lyakhov [3,4] based on a model of perfectly compressible fluids, taking into account the multicomponent composition of the soil. Model of G.M. Lyakhov takes into account the influence of gas trapped in pore water and, as experienced data, well describes the response of water-saturated soils to dynamic load. Blast wave propagation in soil in case of spherical symmetry considered by A.S. Companieyts [11], N.V. Zvolinsky [12], E.I. Shemyakin [13].

More generally, the soil model, as an elastoplastic medium, was proposed by S.S. Grigoryan [14,15]. He adopted a dynamic compression diagram with a load branch at low stresses convex to the pressure axis, and at higher stresses- to the strain axis. Compression chart may have initial linear-elastic section, with a further increase in pressure and part of the bulk deformation proceeds elastically, while the other part plastically. Unloading is only accompanied by reversible changes. density, and the entire branch of unloading is convex to the axis of deformation. In this way, shear deformability in the prelimit state corresponds to the behavior linear elastic medium, and in the limit - Prandtl-Reis scheme with the condition plasticity of Mises-Schleicher-Botkin.

When solving problems of soil interaction with underground structures, widespread model of constraints of finite stiffness. In this model, each constraint determines soil resistance to movement construction in the appropriate direction. Array resistance is set linear, bilinear, piecewise-defined linear, hyperbolic functions, for the constraints are introduced curves "force-displacement".

To assign the rigid characteristics of the constraints use experimental, numerical and engineering methods. The latter are set out in the works of A.B. Einbinder [16], A.G. Kamerstein [17], P.P. Borodavkin [18], V.E. Seleznev [19] and other authors. To date, the dynamic behavior of underground cylindrical structures, taking into account spatial factors when exposed to seismic blast waves, has not been experimentally investigated.

Thus, experimental studies of the effects of seismic blast waves on underground structures (pipelines and tunnels) in soil environments is an urgent task, requiring the development of an experimental technique, as well as the development of adequate mathematical models that meet modern ideas about physical processes in the system “soil-pipeline” and comparison of experimental and theoretical results.

In the explosion of an explosive charge, three zones of its action are distinguished: the plastic zone current and intense compression; zone of elastoplastic deformations and zone elastic deformations [22]. In the framework of this work, a study is made of the behavior of the “soil - pipeline” system in the zone of propagation of elastic seismic waves. The essence of this study is to establish the parameters of seismic vibrations during the explosion of an explosive charge BB, which are acceptable for construction from the conditions of its seismic safety. In every day practice of blasting, the seismic effect of an explosion is evaluated on the basis of the “Unified safety rules for blasting” ПБ 13-407-01, in which, when calculating, the safety criterion is

$$r_c = K_r K_c \alpha^3 \sqrt{Q} \quad , \quad (1)$$

where K_r -coefficient depending on the properties of the soil at the base of the protected facilities; K_c – coefficient, depending on the type of construction and the nature of development; α – explosive factor; Q – charge mass.

This calculation method is used for large industrial explosions, near buildings and structures for industrial purposes, as well as near residential villages. Also, in engineering calculations to determine the appropriate safe distances, the formula has become widespread M.A. Sadovsky [8], obtained on the basis of experimental data:

$$r_c = K_r \sqrt{\frac{Q}{0,4 + 0,6\left(\frac{R_B}{\omega}\right)^3}} \quad , \quad (2)$$

where K_r – soil dependent constant; Q – charge mass, кг; R_B – funnel radius, м; ω – charge depth, м.

Formulas (1), (2) are obtained on the basis of empirical experiments, which certainly affects the accuracy of the results obtained on them. Besides, in they do not take into account the wave pattern of the explosion. The “Building Regulations and Rules (BR and R)“ applicable to trunk pipelines regulate the calculation of pipeline loads taking into account seismic effects from earthquakes, however, seismic effects during blasting operations are of a different nature, local character and more predictable consequences than during earthquakes. With the development of computers and the advent of a large number of software products for calculating the effects of loads on buildings and structures, it became possible to solve the problems of wave action on structures, including pipelines buried in the ground. Using mathematical models of the wave action of the explosion, its

seismic effect can be estimated by the amplitude, speed and period of oscillations of the medium. Many dependencies are known [8,15,16,17] for estimating the amplitude of oscillations, taking into account the depth of the charges, rock properties and the speed of wave propagation. Common to all these dependencies is that they do not take into account a number of factors that significantly affect the assessment of a specific seismic situation. In this regard, the use of vibration amplitude as a criterion for assessing the seismic protection parameters of various structures is limited. A more general criterion for these purposes is the rate of oscillation of the medium in a seismic wave, which for many types of soils, except for water-saturated soils, depends little on the geological conditions of blasting [8]. A direct relationship has been experimentally established between the velocity and the destruction, while this is not observed for the amplitude and acceleration. It is the speed and natural frequency of vibrations of structures that are the main parameters that determine the seismic effect of an explosion on structures. In this regard, in most studies [18, 19, 20], the oscillation velocity is accepted as the main criterion for assessing the seismic effect of explosions. According to the results of experiments [21,22] it was found that the nature soil and pipeline interactions are determined by the state of the soil:

- to a pipeline located in a dispersed water-saturated hoist ground, the explosion acts impulsively. In this case, the maximum displacements and pipeline deformations are observed after the action of a stress wave;
- when the pipeline is located in frozen, rocky or dispersed non-saturated soils, then the pipeline and soil during the explosion move synchronously; the stronger the soil, the closer the parameters and the stricter synchronization of their movement.

2. Methods

2.1 Statement of the problem of theoretical study of seismic blast waves with cylindrical shells

In the soil at a depth there is a concrete cylindrical shell (Fig. 1) with a diameter D , length L and thickness h . At various distances (from the shell), explosives of a spherical shape with a weight of C , kg are laid. To describe the condition of the structure and soils, under the influence of short-term loads, use the methods and laws of two basic theories of solid mechanics: elasticity and plasticity. In solving dynamic problems of soil mechanics, the linear-elastic body model is widely used in the framework of theories of elasticity and plasticity.

Spherical blast wave propagation has been considered in a number of theoretical and experimental work in which the soil was modeled "Plastic gas", an incompressible fluid, elastoplastic and elastic bodies obeying the laws of the theory of plasticity and elasticity and etc. At the same time, the issue of soil model is not settled. Soil model suitable for some conditions, it may be unacceptable in other cases. Couple- meters of soil are poorly studied and unstable. All this provides the basis for the improvement of models.

According to physical and mechanical characteristics and deformation features various types of soils can be distinguished. The need for allocation types of soils due to significant differences in the basic mechanisms deformations of soils, which are most pronounced during explosive loads. Soil behavior is characterized mainly by effects like brittle fracture, loosening of crushed material, cracking, ductility, compaction when exposed to explosive loads, their behavior is highly dependent on the loading speed. We assume that the strains and rotation angles are small, the pipeline material is isotropic and obeys Hooke's linear law. Given these limitations, the stress-strain state of the pipeline is described by the well-known equations of the theory of shells.

The system of three-dimensional equations of the linear theory of elasticity, for dynamic problems of soils, and their behavior is described by the equations

$$\sigma_{ij,j} + \rho_g X_i = \rho_g \frac{\partial^2 u_i}{\partial t^2}; \quad i, j = 1, 2, 3. \quad (3)$$

$$\sigma_{ij} = \lambda_g \theta \delta_{ij} + 2\mu_g \varepsilon_{ij},$$

here X_j - components of the vector of external volumetric forces, u_j - displacement vector components, ρ_g - soil density, δ_{ij} - Kronecker's symbols, λ_g, μ_g - Lamé soil constants.

Based on the review of scientific literature and the analysis of full-scale experiments, we conclude that shell models are the most adequate models describing the process of dynamic deformation of a pipeline [24, 25]

$$L\bar{u} = \frac{(1-\nu_0^2)}{E_0 h_0} \bar{p} + \rho_0 \frac{(1-\nu_0^2)}{E_0} \frac{\partial^2 \bar{u}_0}{\partial t^2}, \quad (4)$$

where

$$L = \begin{pmatrix} \frac{\partial^2}{\partial z^2} + \frac{1-\nu_0}{2R^2} \frac{\partial^2}{\partial \theta^2} & \frac{1+\nu_0}{2R} \frac{\partial^2}{\partial z \partial \theta} & \frac{\nu_0}{R} \frac{\partial}{\partial z} \\ \frac{1+\nu_0}{2R} \frac{\partial^2}{\partial z \partial \theta} & \frac{1+\nu_0}{2} (1+4a) \frac{\partial^2}{\partial z^2} + (1+a) \frac{\partial^2}{\partial \theta^2} & \frac{1}{R^2} \frac{\partial}{\partial \theta} - a(2-\nu) \frac{\partial^3}{\partial z^2 \partial \theta} - \frac{a}{R^2} \frac{\partial^3}{\partial \theta^3} \\ \frac{\nu}{R} \frac{\partial}{\partial z} & \frac{1}{R^2} \frac{\partial}{\partial \theta} - a(2-\nu) \frac{\partial^3}{\partial z^2 \partial \theta} - \frac{a}{R^2} \frac{\partial^3}{\partial \theta^3} & \frac{1}{R^2} + a \left(\frac{\partial^2}{\partial z^2} + \frac{1}{R^2} \frac{\partial^2}{\partial \theta^2} \right)^2 \end{pmatrix},$$

here E_0 – Young's modulus; $\bar{u} = \bar{u}(u, \vartheta, w)$ - displacement vector of the middle surface of the shell (according to the Kirchhoff – Love hypothesis), ν_0 - Poisson's ratio, h_0 - shell thickness, ρ_0 - shell material density, $a = h_0 / (12R^2)$.

So, we consider the system of differential equations (3) - (4), with the corresponding initial and boundary conditions. Until the initial moment of time $t = 0$, the points of the shell and its environment are at rest:

$$\bar{u}_0 = 0, \quad \frac{\partial \bar{u}_0}{\partial t} = 0, \quad u_j = 0, \quad \frac{\partial u_j}{\partial t} = 0, \quad j = 1, 2, 3 \quad (5)$$

At the contact of the shell with the medium ($r = R + h_0 / 2$) the condition of tight adhesion is fulfilled; in this case, the conditions of continuity of stresses and displacements at the layer boundary should be satisfied [24]. Also, boundary conditions are set at the edges of the cylindrical shell. To completely close the statement of the problem, it is necessary to add conditions at infinity to the contact and boundary conditions

$$\bar{u} \rightarrow 0, \quad \text{at} \quad \bar{R} = \sqrt{x^2 + y^2 + z^2} \rightarrow \infty, \quad (6)$$

supplemented by certain radiation conditions. For non-stationary tasks, the causality principle must be fulfilled as a radiation condition: there should be no displacements in the medium outside the region bounded by the leading wave front coming from the vibration sources.

So, let at the initial moment of time the state of the rock mass adjacent directly to the pipeline be known $\vec{U}(0, r, \theta, z) = \vec{U}_0(r, \theta, z)$, where $\vec{U}_0(r, \theta, z)$ - given initial vector. In front of the incident wave $\vec{U}_0(r, \theta, z) = 0$, $\vec{U}_0(r, \theta, z) = (u_{0j}, \sigma_{rro}, \sigma_{\theta\theta o}, \sigma_{r\theta o}, \sigma_{zro})$ - tensor component values $\sigma_{rro}, \sigma_{\theta\theta o}, \sigma_{r\theta o}, \sigma_{zro}$ - stresses at the initial moment of time, u_{0j} - components of the velocity vector at the initial instant of time. Then the values of the stress tensor components behind the wave front are determined by the formulas:

$$\begin{aligned} u_{01} &= -\sigma_0 \cos \theta, \\ u_{02} &= \sigma_0 \sin \theta, \\ u_{03} &= \sigma_0 \cos \theta, \\ \sigma_{rr}^0 &= -\sigma_0 (1 - 2b \sin^2 \theta), \\ \sigma_{r\theta}^0 &= -\sigma_0 (b \sin 2\theta), \\ \sigma_{\theta\theta}^0 &= -\sigma_0 (1 - 2b \cos^2 \theta). \end{aligned} \quad (7)$$

In formulas (7), the value σ_0 sets the distribution of normal voltage behind the front of the incident wave at $t=0$:

$$\sigma_0 = \sigma_{\max}(\bar{r}) e^{-\alpha(\tau - \tau_H)} \sin \beta\tau / \sin \beta\tau_H,$$

where $\sigma_{\max}(\bar{r}) = \rho c \frac{344}{\bar{r}^{1.5}}$ - maximum value of the radial component stress waves; ρc - acoustic rigidity of the rock; $\bar{r} = r / R_z$ - relative distance; r - distance from the axis of charge to the seismic region under study impacts; R_z - charge radius; α - slope rise and fall of voltage amplitude over time; τ - current time with the moment of arrival of the wave at a distance r . τ_H - amplitude rise time stress to maximum; β - coefficient characterizing duration of the positive phase of the stress wave.

When solving various problems, the boundary conditions at the edges of the shell are often not taken into account, i.e. the spatial shell is considered quite long. Then the problem reduces to the plane problem of the theory of elasticity [24,25,26]. Currently, there are many different versions of the theory of plasticity, which differ in the underlying relationships that describe the behavior deformable medium. The two most common theories are distinguished: theory plastic flow and deformation theory of plasticity. When constructing a model of an elastoplastic body, a series of assumptions and admits [12,13], which are based on extensive experimental studies.

So, for example, the strain rate tensor can be represented as the sum of the elastic $\frac{d\varepsilon_{ij}^E}{dt}$ and plastic components $\frac{d\varepsilon_{ij}^P}{dt}$:

$$\frac{d\varepsilon_{ij}}{dt} = \frac{d\varepsilon_{ij}^E}{dt} + \frac{d\varepsilon_{ij}^P}{dt} . \quad (8)$$

In the theory of plastic flow, the relation between increments is accepted plastic deformation and stress deviator components in the form:

$$\frac{d\varepsilon_{ij}^P}{dt} = d\lambda s_{ij} , \quad (9)$$

where s_{ij} - voltage deviator, $d\lambda$ - Prandtl-Reis coefficient, changing during loading: if $d\lambda = 0$, then there is an elastic state; if $d\lambda > 0$ - this is the plastic state of the medium. Using the law of the associated flow and formula (8), expression (9) can be written in the form of the Prandtl-Reis equation:

$$\frac{d\varepsilon_{ij}}{dt} = \frac{1}{2\mu} \frac{ds_{ij}}{dt} + d\lambda s_{ij} , \quad (10)$$

where the derivative is $\frac{ds_{ij}}{dt}$ takes into account the rotation and deformation of a particle of the medium. This

the derivative is calculated in the sense of Jauman – Noll [24]. Equation (8) is supplemented by the Mises flow condition:

$$s_{ij}s_{ij} = \frac{2}{3} \sigma_s^2 , \quad (11)$$

where σ_s – yield strength. Thus, equation (10) together with equations (8) and (9) constitute a closed system of equations, describing the stress deformed state of an ideal elastic plastic material. In the deformation theory of plasticity, the theory of small elastic plastic strains of Genki-Ilyushin, just like in flow theory, the body It is considered isotropic, the relative volume expansion of the medium is elastic. The stress intensity is assumed to be a function of the strain intensity, having the form:

$$\sigma_i = 2m(\varepsilon_i)\varepsilon_i, \quad (12)$$

where $m(\varepsilon_i)$ – a coefficient, depending on the strain intensity is determined according to the results of the experiment. The governing equations, according to this theory [11,12], are represented relations:

$$\sigma_i = 2m(\varepsilon_i)\varepsilon_i + \frac{1}{3}[3K - 2m(\varepsilon_i)]\varepsilon_{kk}\delta_{ij}, K = (3\lambda + 2\mu) / 3. \quad (13)$$

Equations (13) describe the process of elastoplastic deformation at active loading. Thus, the mathematical model considered in the work, describing the adopted scheme (Fig. 1,2), includes defining equations describing the following processes:

- dynamic deformation of the array;
- dynamic pipe deformation.

When developing a mathematical model, a very important issue is determination of the conditions of contact of the “soil-pipeline” system. As a result of numerical integration of the system of resolving equations (3,4,5) we obtain the desired dependences between the tensors of stress and strain. For direct integration of the original differential system second-order partial differential equations developed by mathematical models in the work used the orthogonal sweep method (method of S.K. Godunov [23])

2.2. Experiment Techniques

To study underground structures such as closed-shell cylindrical shells, large-scale field-field experiments were conducted in Uzbekistan and Kyrgyzstan, under the guidance of academician Ya.N. Muborakov [13]. For this, concrete (and steel) thin-walled medium-thickness samples were used, namely, cylindrical closed-profile samples of the following sizes: steel sample $L = 6.0$; $D_H = 0.72$ m, $\delta = 0.008$ m. (L – steel sheath length; D_H – shell diameter, δ – shell thickness).

The scheme of layout of devices is shown in Fig. 1. Seismic receivers for fixing vibrations of the “soil-structure” system were installed (fixed) directly on a concrete base without special fastening, since only small vibrations were measured.

To maximize the description of the physical nature of the interaction during the experiments, along with seismometric observations, tensometric observations were simultaneously carried out. The arrangement of strain gauges and pressure sensors on cylindrical samples of open and closed profiles is shown in Fig. 2. Site preparation and laying of samples was carried out in accordance with regulatory documents for laying similar structures used in network underground structures in highly seismic regions.

To effectively determine the dynamic behavior of the soil and the sheath, the displacements of the structure, soil, and loads incident on the underground pipe (sheath) simultaneously in three mutually perpendicular directions were measured (Fig. 1). Records of longitudinal, transverse and vertical displacements of a cylindrical structure (pipe) at points 1 and 2 were obtained, and at a point 3 — longitudinal displacement, speed and acceleration (Fig. 1). The recording of displacement, speeds and accelerations, oscillations was carried out using galvanometers, respectively types $\Gamma\text{B-III-B-5}$, $\Gamma\text{B-III-B-10}$, and $\Gamma\text{B-IV-B-3}$ installed in the loop oscilloscopes H-700 (H-041). Signals from strain gauges and pressure sensors were recorded on H-117/1 (H-115) oscilloscopes using type M 1005 and M 017 galvanometers. The oscilloscopes were started using special starting devices that simultaneously triggered all oscilloscopes and produced an explosion, as well as automatic stop after attenuation of the oscillatory process. Based on the capabilities used in excavation (digging) work, the samples were laid to a depth of 2.5 m to 5.0 m from the surface of the earth, then geophones, sensors and strain gauges were installed and tested for sensitivity and operability from compensation elements, which made it possible to close the system for measuring the effects of seismic blast waves.

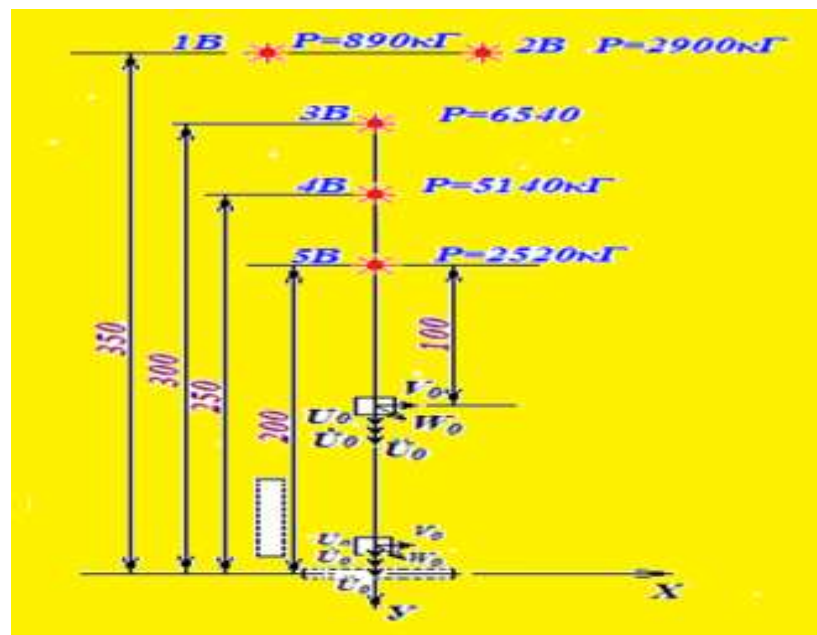


Fig. 1. The scheme of layout of the tested structures on the experimental site relative to the explosion points

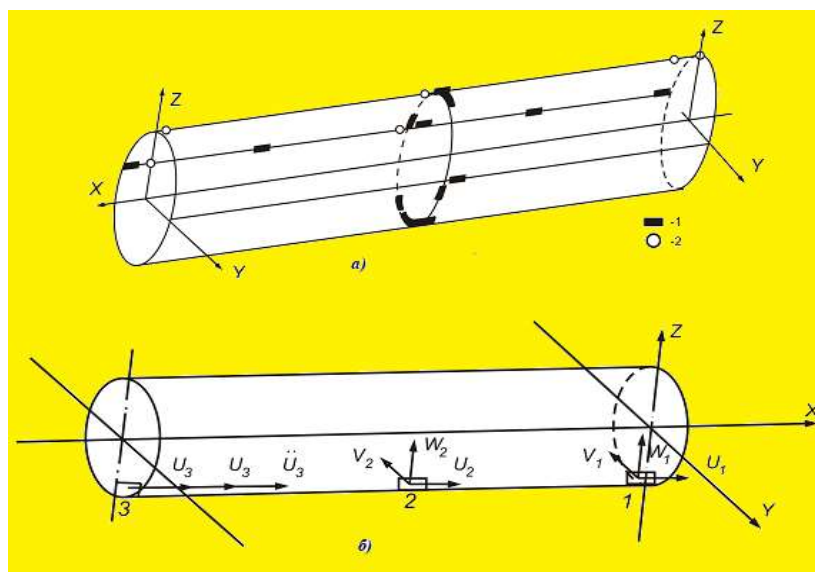


Fig. 2. Arrangement of strain gauges and pressure sensors (a), as well as geophones (b) on a cylindrical sample: 1-strain gauges for measuring annular and longitudinal deformations; 2-pressure sensors

The technology of preparation, calibration and measurement was carried out on the basis of [13]. After removing all the necessary characteristics of the strain gauge and seismometric channels, the trenches were manually filled with a thickness of 0.2-0.4 m., each time with the sinus densified, then the trench was filled (after 3.0 m of the manual filling) with a bulldozer, after filling, the data was zeroed out objects.

The spectra of vibrations of soil and underground structures excited by underground explosions differ from the spectra of vibrations of natural tectonic earthquakes. High frequencies prevail in them. The amplitude of the oscillations, as a rule, does not exceed a few millimeters. Therefore, to record such oscillations, VEGIK, SM-2, SM-3, S-5-S and other seismometers were used, corresponding equipment with wide frequency response ranges.

At the investigated objects (structures) and adjacent sections of the soil environment, displacements were measured u_i, v_i, w_i , speeds $\dot{u}_i, \dot{v}_i, \dot{w}_i$ and accelerations $\ddot{u}_i, \ddot{v}_i, \ddot{w}_i$, in directions Ox, Oy, и Oz (Fig. 1). The study of the influence of the elastic properties of the soil on the vibrations of the structure, during their joint oscillation, is complicated due to the phenomenon of the reverse effect of the vibrating structure on the surrounding soil. The inertia forces of a massive structure, set in motion by environmental vibrations, in turn, cause fluctuations in the soil adjacent to the structure. As a result, the motion of the soil surrounding the structure

does not follow the oscillations of the earth's crust. This phenomenon was observed during many earthquakes (for example, in Tokyo, 1923)..

The result of this phenomenon can be a significant decrease in the inertia forces acting on the structure during an earthquake. Therefore, during field experiments, the geophones were installed at a distance of 3.0 m from the points of the construction location. Explosions of the ground during explosions were recorded at two points: No. 1 (control point) and No. 2 (main observation point), the distance between which is 100 m. At point No. 1 (control point), displacement (u) in the longitudinal direction, speed of displacement (\dot{u}) and acceleration of oscillation (\ddot{u}), also in the longitudinal direction were recorded. At point 2 (the main observation point), motions were also recorded in three mutually perpendicular directions (u, v, w), velocity of displacement (\dot{u}) and acceleration (\ddot{u}) in the longitudinal direction (Fig. 1). As indicated above, measurements of seismic explosive vibrations of the soil were carried out using seismographs and oscilloscopes. The sensors used were pendulum-type geophones with a magneto-electric transducer and adjustable magnetic attenuation ВЭГИК, ОСП-Г and С-5-С. To record the bias, we used, in conjunction with the С-5-С and ВЭГИК, seismometers, miniature mirror frame galvanometers of the ГБ – III brand, which were in a rested mode and, as a result, integrated the currents entering them in a certain frequency range. Galvanometers have a natural frequency of 5 Hz. To record the speed and accelerate the displacement of soil vibrations, the ВЭГИК and ОСП-Г seismometers were used together with ГБ-IV galvanometers with a natural frequency of 120 Hz. Vibrational motion of the soil was recorded on oscillographic photo paper 120 mm wide, and sensitivity of 800-1000 units. Draw speed - 640 mm / s.

During field observations, all oscilloscopes were mounted in a carriage, which was supported by shock absorbing supports, in order to eliminate the interference caused by sharp swings during explosions.

Since the main explosions and shootings made were very different in weight, and the recorded seismic vibrations of the soil belong to different distances from the observation point to the explosion point, we will use the following parameter to compare the results of observations with each other:

$$R_{\text{np}} = R / \sqrt[3]{C} \quad [M \cdot kT^{-1/3}] \quad , \quad (14)$$

representing the reduced distance where all charges are expressed in kilograms, and the distance from the point of explosion to the observation point is in meters. When studying the dynamics of the wave process (amplitudes and periods of seismic blast waves, their spectra, etc.), where seismic instruments are used, it is impossible to

obtain the true values of the above parameters without having a sufficient value of the frequency characteristics and sensitivity of the instruments used.

Thus, the connection with the accumulation of a large amount of accumulated experimental research material in the considered area of earthquake resistance of underground structures can be considered very effective, where the use of modern computer technology makes it possible to interpret almost any results. In connection with the prospects of the seismic-explosive research method, due to their high cost-effectiveness and reliability of the results, when assessing the seismic stress state of an underground structure interacting with an energy-bearing medium, it seems relevant in a scientific aspect and in a practical application.

In a similar formulation, problems are solved theoretically. The obtained analytical and experimental calculation results are compared.

2.3 Numerical schemes and algorithms for studying the dynamic behavior of cylindrical shells when exposed to seismic blast waves

So, the process of dynamic deformation of the “soil-pipeline” system can be described by the well-known equations of continuum mechanics in an axisymmetric formulation in Euler variables [27]. In connection with the linearity of the problem statement, we seek the solution of partial differential equations in the form:

$$\vec{U} = \sum_{n=0}^{\infty} \vec{U}_{kn}(r, z, t) \Phi_n(\theta), \vec{U}_0 = \sum_{n=0}^{\infty} \vec{U}_{0n}(R, z, t) \Phi_n(\theta), \quad (15)$$

Where τ_1, U_n, V_n, W_n - amplitudes of displacements, n - integers, $\vec{U}_0 = \{U_{0n}, V_{0n}, W_{0n}\}^T$.

Substituting (15) into (3) - (6), we obtain the following system of partial differential equations in displacements

$$\begin{aligned} & \frac{\lambda_c + 2\mu_c}{\mu_c} \left(\frac{\partial^2 W_n}{\partial r^2} + \frac{1}{r} \frac{\partial W_n}{\partial r} - \frac{W_n}{r^2} \right) + \frac{\lambda_c + \mu_c}{\mu_c} \left(\frac{\partial^2 U_n}{\partial r \partial z} + \frac{n}{r} \frac{\partial V_n}{\partial r} \right) - \\ & - \frac{n^2}{r^2} W_n + \frac{\partial^2 W_n}{\partial z^2} - \frac{(\lambda_c + 3\mu_c)n}{\mu_c r^2} V_n = \frac{\rho_s c_0^2}{\mu_c} \frac{\partial^2 W_n}{\partial t^2}, \\ & \frac{\partial^2 V_n}{\partial r^2} + \frac{1}{r} \frac{\partial V_n}{\partial r} - \frac{(\lambda_c + \mu_c)n}{\mu_c r} \left(\frac{\partial W_n}{\partial r} + \frac{\partial U_n}{\partial z} \right) - \frac{V_n}{r^2} - \\ & - \frac{\lambda_c + 2\mu_c}{\mu_c r^2} n^2 V_n + \frac{\partial^2 V_n}{\partial z^2} - \frac{(\lambda_c + 3\mu_c)n}{\mu_c r^2} W_n = \frac{\rho_s c_0^2}{\mu_c} \frac{\partial^2 V_n}{\partial t^2}, \\ & \frac{\partial^2 U_n}{\partial r^2} + \frac{1}{r} \frac{\partial U_n}{\partial r} + \frac{\lambda_c + \mu_c}{\mu_c r} \left(\frac{\partial W_n}{\partial z} + n \frac{\partial V_n}{\partial z} + r \frac{\partial^2 W_n}{\partial r \partial z} \right) - \frac{n^2}{r} U_n + \\ & + \frac{\lambda_c + 2\mu_c}{\mu_c} \frac{\partial^2 U_n}{\partial z^2} = \frac{\rho_s c_0^2}{\mu_c} \frac{\partial^2 U_n}{\partial t^2}, \end{aligned}$$

$$\bar{L}_n \bar{u} = \frac{(1-\nu_0^2)}{E_0 h_0} \bar{P}_n + \rho_0 \frac{(1-\nu_0^2)}{E_0} \frac{\partial^2 \bar{u}_0}{\partial t^2},$$

$$\bar{L}_n = \begin{pmatrix} \frac{\partial^2}{\partial z^2} - \frac{1-\nu_0}{2R^2} n^2 & -\frac{1+\nu_0}{2R} n \frac{\partial}{\partial z} & \frac{\nu_0}{R} \frac{\partial}{\partial z} \\ -\frac{1+\nu_0}{2R} n \frac{\partial}{\partial z} & \frac{1+\nu_0}{2} (1+4a) \frac{\partial^2}{\partial z^2} - (1+a) n^2 & -\frac{1}{R^2} n + a(2-\nu) n \frac{\partial^2}{\partial z^2} - \frac{a}{R^2} n^3 \\ \frac{\nu_0}{R} \frac{\partial}{\partial z} & -\frac{1}{R^2} n - a(2-\nu) n \frac{\partial^2}{\partial z^2} - \frac{a}{R^2} n^3 & \frac{1}{R^2} + a \left(\frac{\partial^2}{\partial z^2} - \frac{1}{R^2} n^2 \right)^2 \end{pmatrix}, \quad (16)$$

where λ_c, μ_c - Lamé coefficients (16). The problem is solved in dimensionless quantities. As the length scale, the outer radius R of the cylinder is used, and the time scale - R/c_0 . The components of the displacement vector are related to $p_0 R / \mu_k$.

Solution of (16), taking into account the boundary and initial conditions (5) and (6), is carried out by the finite difference method. Region $0 \leq r \leq R$ split into N segments h_r ($h_r = R/N$), and exposure time - in small steps τ . For considering various versions of the problem, it was assumed that $N = 40$; J depended on the time interval in which numerical integration was performed. At each internal point of the medium i ($i = 3, 4, \dots, N+1$) at times $t = (m-2)\tau$ ($m = 2, 3, \dots, J$) equation (1) was written in finite differences. To calculate the cylindrical shells in an elastic medium under the influence of seismic blast waves, a difference scheme is used [28]. In the nodes lying inside the elastic cylindrical region, partial derivatives are represented using central differences of the form

$$\frac{\partial W(r_i, t)}{\partial r} = \frac{1}{2h_r} (W_{i+1}^m - W_{i-1}^m) + O(h_r^2);$$

$$\frac{\partial^2 W(r_i, t)}{\partial r^2} = \frac{1}{h_r^2} (W_{i+1}^m - 2W_i^m + W_{i-1}^m) + O(h_r^2);$$

$$\frac{\partial W(r_i, t_m)}{\partial t} = \frac{1}{2\tau} (W_i^{m+1} - W_i^{m-1}) + O(\tau^2);$$

$$\frac{\partial^2 W(r_i, t_m)}{\partial t^2} = \frac{1}{\tau^2} (W_i^{m+1} - 2W_i^m + W_i^{m-1}) + O(\tau^2); \quad (17)$$

$$\frac{\partial^4 W(r_i, t)}{\partial r^4} = \frac{1}{h_r^4} (W_{i+2}^m - 4W_{i+1}^m + 6W_i^m - 4W_{i-1}^m + W_{i-2}^m) + O(h_r^2).$$

Here $W_i^m, \dots, W_{i-2}^m, W_i^{m+1}$ - grid functions; r_i - node coordinate on the line r ; other functions $V_i^m, \dots, V_{i-2}^m, V_i^{m+1}$ - are written in a similar form (17). Difference approximations of derivatives with respect to r have the same (second) order of accuracy with respect to h_r , accuracy of approximation of derivatives with respect to time of the order τ^2 . In the nodes lying inside the

viscoelastic region, using the central differences of the form (17), we write an explicit approximation of the equations defining w_k, ϑ_k, u_k :

$$\begin{aligned}
 U_{i,j}^{m+1} &= 2U_{i,j}^m + U_{i,j}^{m-1} + c_1 [U_{i,j+1}^m - 2U_{i,j}^m + U_{i,j-1}^m + c_2 (U_{i,j+1}^m - U_{i,j-1}^m)] - \\
 &- c_3 U_{i,j}^m + c_4 (U_{i+1,j}^m - 2U_{i,j}^m + U_{i-1,j}^m) + c_5 (V_{i+1,j}^m - V_{i-1,j}^m) + c_6 (W_{i+1,j}^m - W_{i-1,j}^m) + \\
 &+ c_7 (W_{i+1,j+1}^m - W_{i-1,j+1}^m - W_{i+1,j-1}^m + W_{i-1,j-1}^m); \\
 V_{i,j}^{m+1} &= 2V_{i,j}^m - V_{i,j}^{m-1} + c_1 [V_{i,j+1}^m - 2V_{i,j}^m + V_{i,j-1}^m + c_2 (V_{i,j+1}^m - V_{i,j-1}^m)] - \\
 &- c_8 V_{i,j}^m + c_9 (V_{i+1,j}^m - 2V_{i,j}^m + V_{i-1,j}^m) - c_{10} W_{i,j}^m - c_{11} (W_{i,j+1}^m - W_{i,j-1}^m) - c_5 (U_{i+1,j}^m - U_{i-1,j}^m); \\
 W_{i,j}^{m+1} &= 2W_{i,j}^m - W_{i,j}^{m-1} + c_{12} [W_{i,j+1}^m - 2W_{i,j}^m + W_{i,j-1}^m + c_2 (W_{i,j+1}^m - W_{i,j-1}^m)] - \\
 &- c_{13} W_{i,j}^m + c_9 (W_{i+1,j}^m - 2W_{i,j}^m + W_{i-1,j}^m) + c_{11} (V_{i,j+1}^m - V_{i,j-1}^m) + c_7 (U_{i+1,j+1}^m - U_{i-1,j+1}^m - \\
 &- U_{i+1,j-1}^m + U_{i-1,j-1}^m) - c_{10} V_{i,j}^m.
 \end{aligned} \tag{18}$$

Here

$$\begin{aligned}
 c &= (\lambda_1 + 2\mu_1) / \mu_1; c_1 = \mu_1 \tau^2 / \rho h_r^2 a_0^2; c_2 = 0.5 / (1 / h_r - j + 1); c_3 = 4k^2 c_1 c_2^2; c_4 = c h_r^2 h_x^{-2}; \\
 c_5 &= (c - 1) k h_r h_x^{-1} c_1 c_2; c_6 = c_5 k^{-1}; c_7 = c_6 c_2^{-1} / 4; c_8 = 4(c k^2 + 1) c_1 c_2^2; c_9 = c_1 h_r^2 h_x^{-2}; \\
 c_{10} &= 4(c + 1) k c_1 c_2^2; c_{11} = (c - 1) k c_1 c_2; c_{12} = c c_1; c_{13} = 4(c + k^2) c_1 c_2^2.
 \end{aligned}$$

When implemented on a computer, an explicit three-layer scheme for approximating time derivatives with a constant step was used h_t [28]. To obtain a difference analog of spatial derivatives, the computational domain $r_0 \leq r \leq R$, $0 \leq z \leq L$ covered with a grid, consisting of quadrangular elements with sides h_r and h_z . Here, an algorithm for outputting results in the fields of equal stress lines relative to variables is implemented. r and z at $\varphi = const$ and the desired sequence of points in time. At the same time, processing the results consists in analyzing the development of stresses over a set of flat patterns of stress isolines. The main result of this data presentation is a significant reduction in the time of the entire study. The solution was limited to five members of the Fourier series (15), since for a given load change (18), holding the next member of the series, almost 10 members, changes the amplitude value of the voltage by less than 3%. The time step is determined from the Courant condition. Further refinement h_t carried out in the calculation process. To solve the problem, step in time selected $h_t = 2 \cdot 10^{-5} c$.

3. Results and discussions

According to the results of laboratory studies, it was found that the content of fine sand in the soil was about 21.4%, dust particles -46.2%, clay-25.6%. High salinity of the medium was found to be quite satisfactory; at a depth of 2.0 m from the surface, the fractions of the medium are more evenly distributed: for

sand with a particle diameter of 1.00 ... 0.05 mm it is 21-29%, dusty fractions (0.05-0.005 mm.) - 47-53%, clay (0.005-0.002) -13-28%. Maximum humidity ranges from 16% to 21%. The number of ductility varies between 7-18, at a depth of 2.0 m. it is equal, on average, 0-11. Natural soil moisture in the 0-2.0 m layer varied from 16.2% to 22%. Soils turned out to be the wettest at a depth of 2.0 m. In order to approximate the soil structure in the trenches where the test structure is located, backfilling is recommended manually and every 0.15-0.40 m (depending on soil conditions) the thickness and soil are compacted . It should be noted here that, backfilled soil does not get a natural structure in a short time. Taking into account the increment of score due to groundwater (with a depth of groundwater of 10 m or more), a change in depth does not affect the intensity within the upper 10 meter thickness.

Figures 3 and 4 show a series of records of the speed of seismic explosive vibrations of the soil for different reduced distances ($R_{np} = 14,5 \div 24,54$). The waveforms shown here refer to the longitudinal component of the velocity. If we consider the records of the speed of soil vibrations, we note that the initial, relatively simple in form signal, is observed at small reduced distances. Points that are the foundations of structures always have a more or less clearly defined layered structure. As a result of this, in addition to the direct waves reaching the observation point, along the shortest distance, waves reflected by different layers propagate in the soil, which have time to interact with the layers and interfering with the direct waves, significantly complicate the general nature of the movement of the soil. The above description of the movement of the soil at large reduced distances from the point of explosion is confirmed by the distance, waves reflected by different layers propagating in the soil, which have time to interact with the layers and interfering with direct waves, propagate in the soil, significantly complicating the general nature of the movement of the soil. The above description of the movement of the soil at large reduced distances from the explosion point is confirmed by a complex oscillation train, which contains several peaks and troughs of different amplitudes and then fades out smoothly. Peak value corresponding to maximum, on the recording, the oscillation is observed some time after the start of the oscillation, i.e. the change in speed in such vibrations is smooth, not shock. If we consider the vibrations of the soil at various reduced distances, we can see that the maximum peak, as in the mixing record, mixes with the increase in the reduced distance towards the end of the record. So, in experiments No. 3 and No. 4, at the control point, the peak is observed for the first movement, and in subsequent experiment No. 2, at the control point, it is no longer in the middle, and at large reduced distances of experiment No. 3 and experiment No. 2, at the main observation point, the maximum peak moves to end of recording.

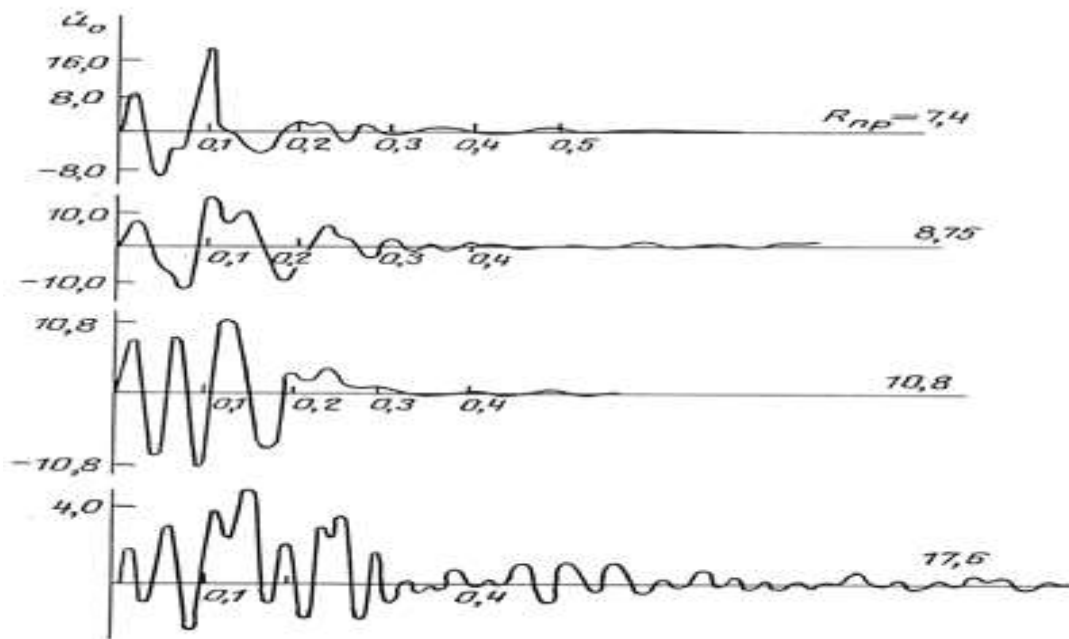


Fig. 3. The speed of soil particles at various reduced distances (fixed at a control point, near explosion point)

Thus, the initial simple seismic-explosive signal, which is observed in the form of a complex train of oscillations, where several peaks and valleys of different amplitudes are visible. On the record-oscillograms, in addition to the first introductions, one can notice the development of individual characteristic phases. According to these data, based on the values of speed and displacements, hodographs were built. In addition, with an increase in the reduced distance, an increase in the duration of the oscillations is observed. If we compare the records of different reduced distances, we note that for large reduced distances, the duration is longer than for the others. Pay attention to the "density" of records, i.e. the number of peaks on the head. Here we see that at different reduced distances the number of peaks is different, with an increase in the reduced distance, the "density" of the number of oscillations increases, and the damping becomes smoother. The calculation results of the logarithmic attenuation decrements show that the attenuation at the control point, i.e. in close proximity to the explosion point, more than at the main observation point. It follows that with an increase in the reduced distance, the values of the logarithmic attenuation decrements decrease. The amplitude of the speed of movement of the soil at small reduced distances is characterized by significant values. With increasing distance, these amplitudes become rapidly attenuated

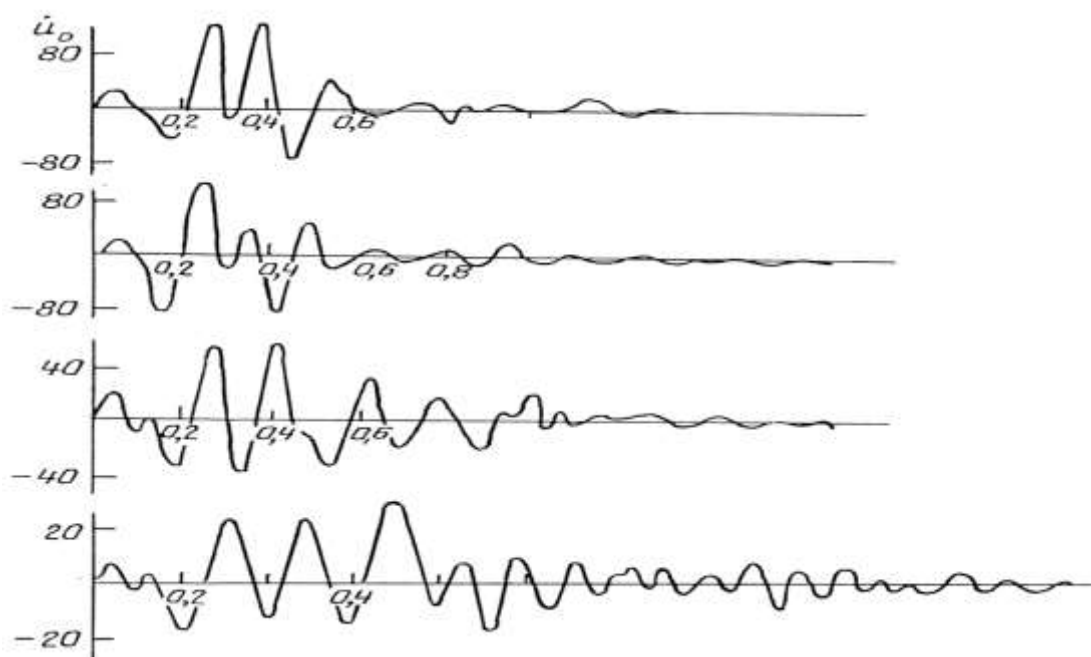


Fig. 4. The speed of soil particles at various reduced distances (recorded at the main observation point)

An analysis of the displacement and velocity waveforms (Figs. 3 and 4) shows that the maximum values of the velocity in time do not agree with the maximum displacement of the same point of the soil, in all experiments the displacement reaches its maximum earlier than the velocity. In addition, the range of the head of the velocity is wider than the displacement of the soil at the same point, and the amplitude of the velocity is not always proportional to the maximum mixing in the soil. An analysis of the obtained experimental results showed that the rise time of normal stresses in the array to a maximum τ_1 little changes depending on the distance and weight of the explosive charge. Value τ_u characterizing the duration of the load increases with the weight of the explosive charge BB [34,35]. Below (Fig. 5) are the experimentally obtained results of the time of the rise in speed to the maximum and the duration of the seismic explosive load.

These results (Fig. 3) were obtained for large-scale field underground explosions by experimental research and is used as an external load to solve the problems theoretically.

The location of the measuring site of the rock is represented by granite density 2590 кг/м^3 , Young's modulus $-5,74 \cdot 10^{10}$, Poisson's ratio of -0.18 . The results of measurements of annular stresses in the pipeline wall, versus time, at points 1-3 (Fig. 6), are presented in Fig. 7 – 11 [36,37].

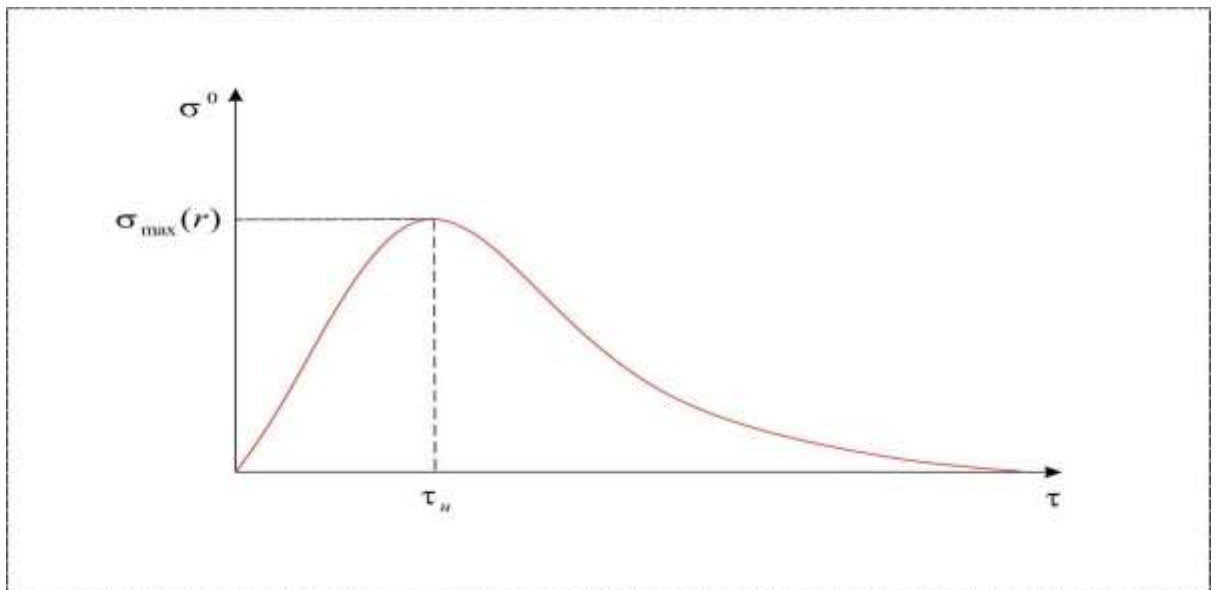


Fig. 5. The dependence of the normal stresses in the array on time at boot

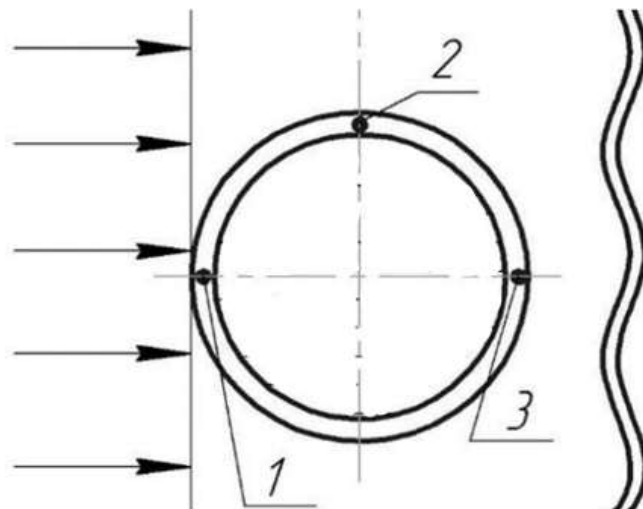


Fig. 6. The design scheme

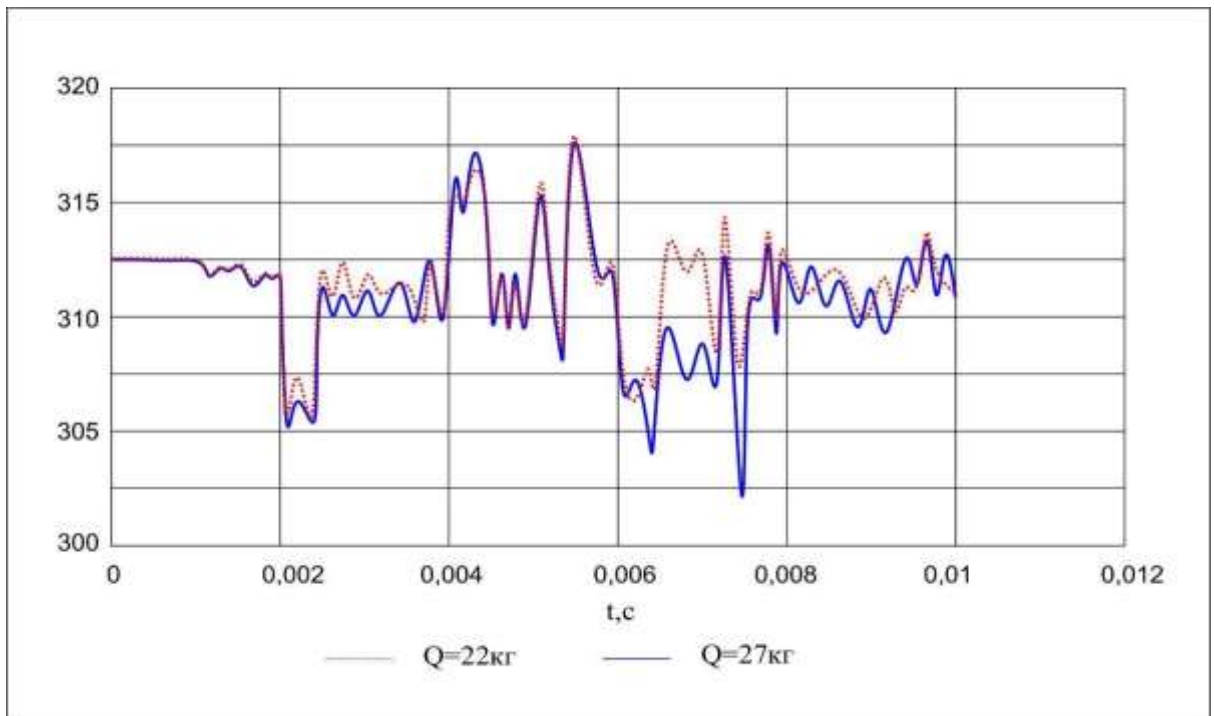


Fig. 7. The dependence of ring stresses in the wall of the pipeline on time at point 1

The pipe is made of reinforced concrete and steel: $E_g = 6.67 \cdot 10^4 \text{ MPa}$,

$\nu_g = 0.2$, $\rho_g = 2280 \text{ kg} / \text{m}^3$.

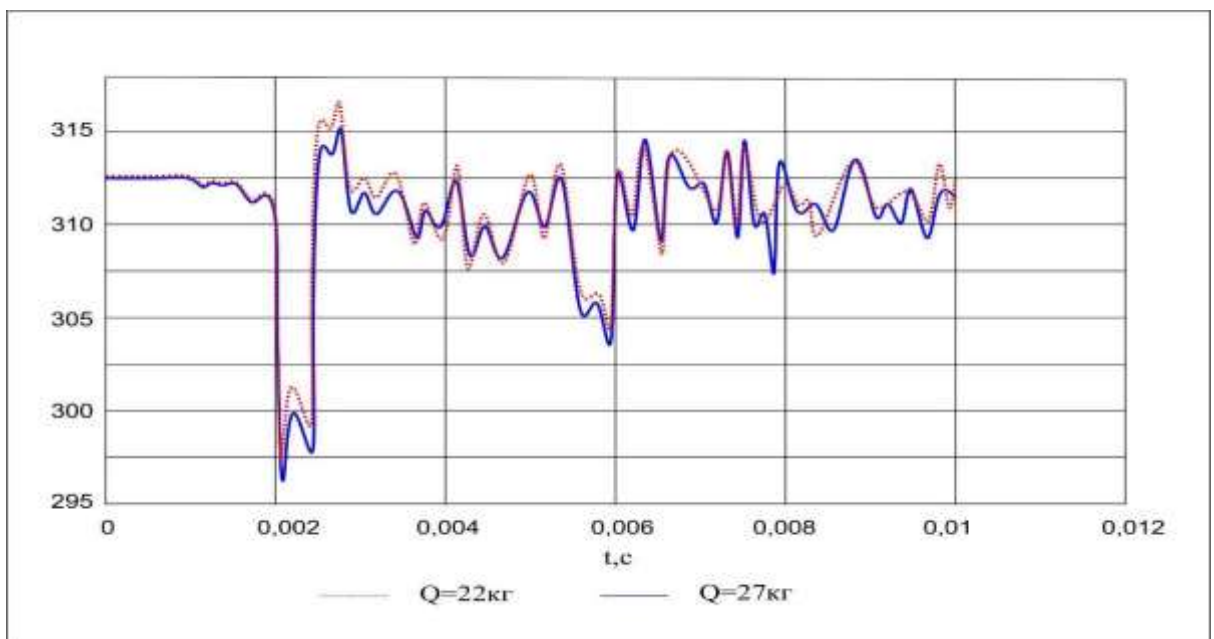


Fig. 8. The dependence of ring stresses in the wall of the pipeline on time at point 2

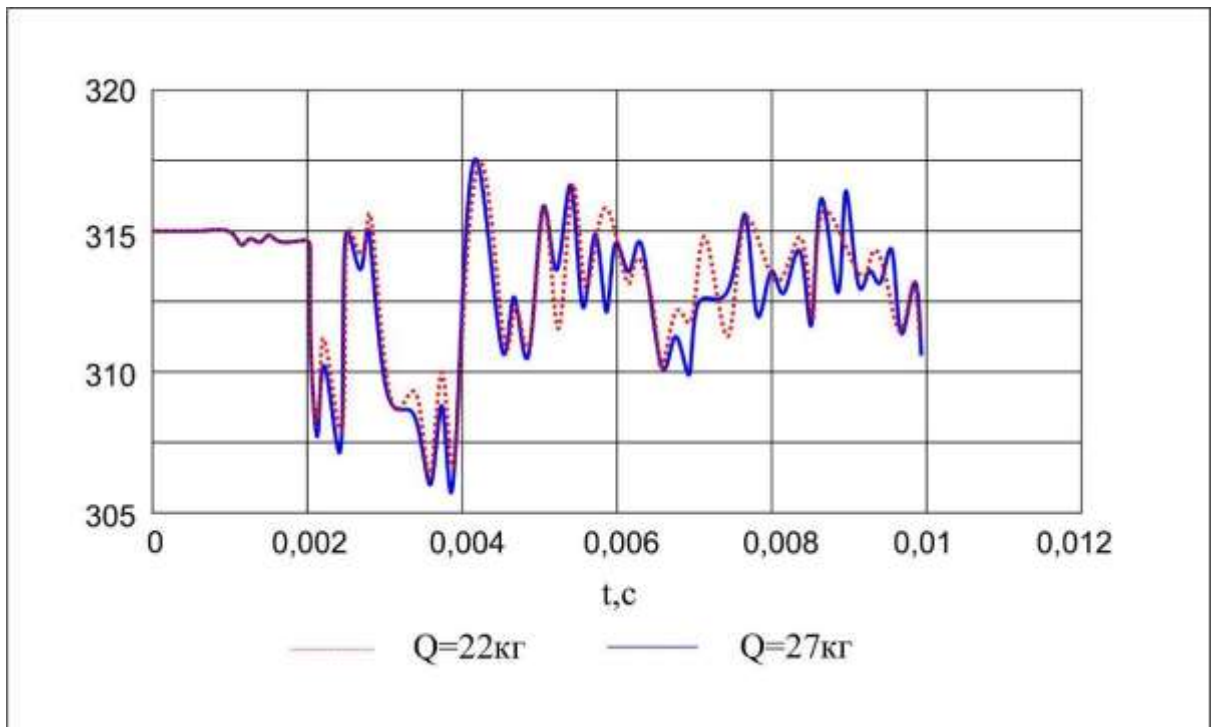


Fig. 9. The dependence of ring stresses in the wall of the pipeline on time at point 3.

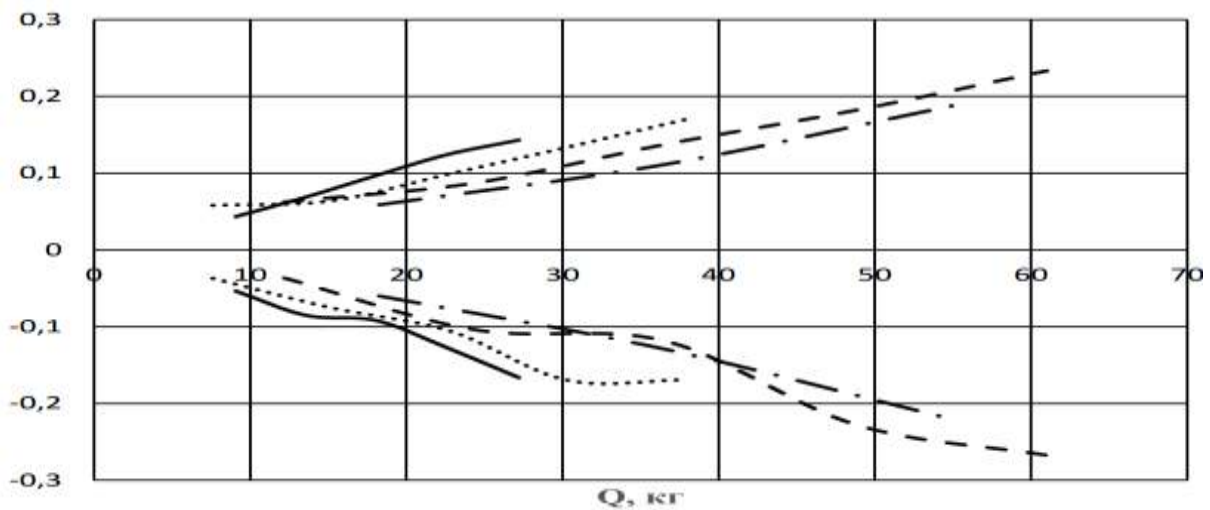


Fig. 10. The dependence of the extreme values of the radial components of the velocity vectors on the mass of the charge at point 1

- | | | | |
|-------|-------------------------------------|-----------|--------------------------------------|
| ————— | $V_{\text{max}}, d = 65 \text{ mm}$ | ----- | $V_{\text{max}}, d = 90 \text{ mm}$ |
| ————— | $V_{\text{min}}, d = 65 \text{ mm}$ | ----- | $V_{\text{min}}, d = 90 \text{ mm}$ |
| | $V_{\text{max}}, d = 75 \text{ mm}$ | - · - · - | $V_{\text{max}}, d = 100 \text{ mm}$ |
| | $V_{\text{min}}, d = 75 \text{ mm}$ | - · - · - | $V_{\text{min}}, d = 100 \text{ mm}$ |

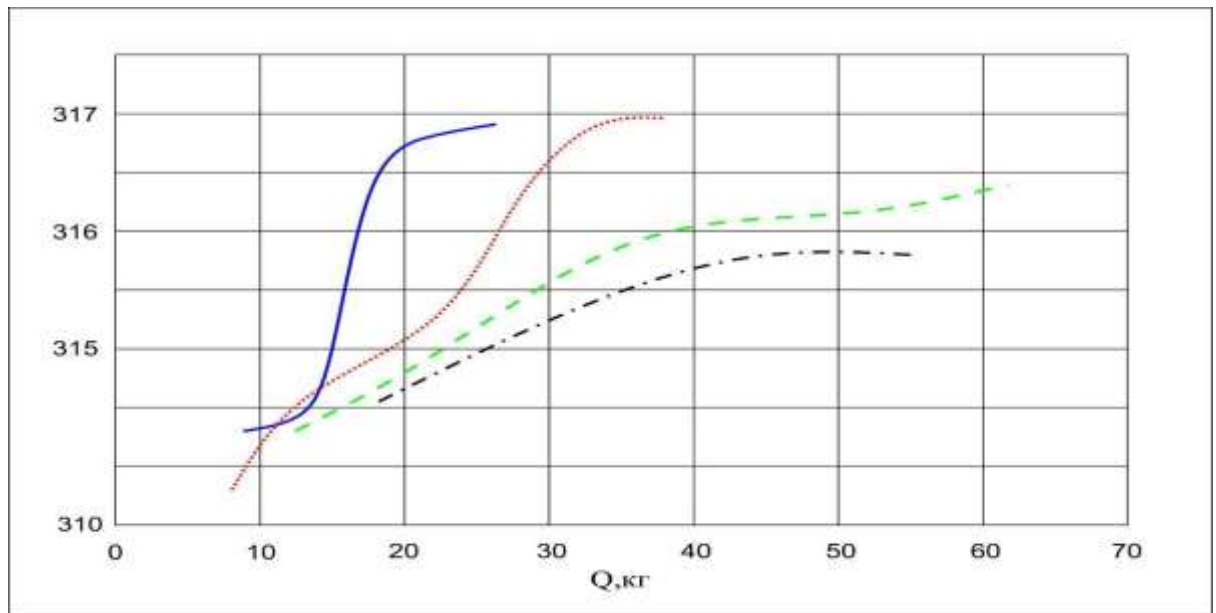


Fig. 11. The dependence of the resulting maximum stresses in the wall of the pipeline from the mass of the explosive charge BB

—————	d = 65 mm	— — — — —	d = 90 mm
.....	d = 65 mm	- · - · - ·	d = 90 mm

In experiment with charge diameters of 75 mm (Fig. 9 and 10), the maximum modulus of the radial components of the velocity vectors displacements take values of 0.17 m / s and 0.18 m / s at points 1 and 2, tangential components - 0.18 m / s and 0.14 m / s at points 2 and 3. Maximum stresses in the wall pipelines arise at point 1 (316 MPa) with a charge mass of 37.9 kg. The maximum values of the components of the displacement velocity vectors and the values maximum stresses from the second experiment are comparable with the results the first experiment and take equal values (the difference is 0.01 m / s).

As a result of a series of numerical experiments with gradually increasing masses and diameters of charges it was found that stresses in the oil pipeline (oil pipeline diameter 1000 mm, wall thickness 14 mm, oil pressure 9 MPa) begin to approach the maximum level permissible stresses of 317 MPa (taking into account the safety factor 1.15 for pipeline) with a total mass of charges of 27 kg and well diameters of 64 mm, and also with a total mass of charges of 38 kg and diameters of 76 mm. The use of explosive charges with a diameter of 89 mm and 102 mm allows for the simultaneous explosion of explosive charges weighing up to 60 kg. An analysis of the relationship between stresses and velocities of the displacement of the wall of the pipeline shows that with an explosive charge mass of 27 kg and a diameter of 64 mm, the velocity of the displacement of the wall of the

pipeline is 0.15 m / s, and the stresses approach the maximum allowable. However, with an explosive charge mass of 50 kg and a diameter of 90 mm, the displacement rate of the pipeline wall reaches 0.3 m / s, and the stress values remain unchanged. Further, for comparative analysis, the results of numerical simulation of the effect of a seismic blast wave on an array (Fig. 11) with the same parameters of large-scale explosive experiments as with field measurements. The solid and broken lines represent the experimental results. The figure shows that the experimental and theoretical results differ with differences of 25-40%.

It should be noted that at distances greater than $150 R_{\text{zap}}$, the effect of the charge length on the amplitude of the stress wave ceases when the charge length is more than $50 R_{\text{zap}}$ [36]. That is, a further increase in the mass of the charge "in depth" will not change the amplitude of the stress wave, and accordingly the amplitude of the seismic wave at the point of measurement. In the process of numerical simulation it was found that an increase in the mass of the explosive charge occurs as a result of an increase in the number of simultaneously exploded charges in the deceleration stage. Comparing the results of measurements of the components of the soil displacement velocity vectors during field tests with the results of a numerical experiment, we note that three measurements were made with a charge mass of 8 kg, the results of which are in the range of 3-5 cm / s for both the radial and tangential components of the velocity vectors. These results are comparable with the results of a numerical experiment.

4. Conclusions

The general kinematic and dynamic signs of seismic blast waves and the parameters of the process of interaction and movement of the soil medium, the establishment of which is possible on the basis of this research methodology, allow us to establish correlations between the process of interaction and movement of media during seismic explosive influences with the parameters of seismic blast waves. Experimental research methods are still the main scientific source of benign information about the seismic stress state of underground structures. Judging by the scientific periodicals, research teams have accumulated considerable experimental material. Currently, the urgent task of experimenters is to create publicly accessible databases based on its systematization and synthesis of materials.

Reference

1. Sadovsky M.A. (1920) Assessment of seismically hazardous zones during explosions. Transactions Seismological Institute of the Academy of Sciences of the USSR. 106: 6-16.
2. Sadovsky M.A., Kostyuchenko V.N.(1974) About the seismic action of underground explosions. Reports of the USSR Academy of Sciences. 215, 5: 1097-1100

3. Lyakhov G.M., Polyakova N.I. (1967) Waves in dense media and loads on facilities. Moscow, Nedra
4. Lyakhov G.M. (1974) Fundamentals of the dynamics of blast waves in soils and rocks. Moscow, Nedra
5. Adushkin V.V., Spivak A.A. (1993) Geomechanics of large explosions. Moscow, Nedra
6. Rodionov V.N., Adushkin V.V., Kostyuchenko V.N., Nikolaevsky V.N., Romashov A.N., Tsvetkov V.M. (1971) The mechanical effect of an underground explosion. Moscow, Nedra
7. Kutuzov B.N. (2009) Blasting safety in mining and industry. Moscow, Mountain Book
8. Medvedev S.V. (1964) Seismic of mountain explosions. Moscow: Nedra
9. Equist B.V., Bragin P.A. (2009) Explosive seismic impact assessment Work on the Environment and Protected Objects: A Training Manual for universities. Moscow, MGGU
10. Gospodarikov A.P., Gorokhov H.L. (2011) Dynamic calculation of pipelines on seismic effects. Notes of the Mining Institute. 193: 318- 321
11. Kompaneyets A.S. (1956) Shock waves in a plastically compacted medium. Dokl. USSR Academy of Sciences.. 109, 1: 49-52
12. Zvolinsky N.V. (1954) Multiple Reflections of Elastic Waves in a Layer. Transactions Geophysis. Institute of Academy of Sciences of the USSR. 22: 26-49
13. Shemyakin E.I. (1968) Dynamic problems of the theory of elasticity and plasticity. Novosibirsk, NSU
14. Grigoryan S.S. (1960) On the basic concepts of soil dynamics 24, 6: 1057-1072
15. Grigoryan S.S. (1967) Some questions of the mathematical theory of deformation and destruction of hard rocks. J Prikl Math and Mech 31 4: 634-649.
16. Ainbinder A.B. (1991) Calculation of trunk and field pipelines for strength and stability. Moscow, Nedra
17. Kamerstein A.G., Rozhdestvensky V.V., Ruchimsky M.N. (1963) Payment Piping Strength: A Reference Book. Moscow, Gostoptekhizdat
18. Borodavkin P.P. (2003) Soil mechanics. Moscow, Nedra-Business Center
19. Seleznev V.E., Aleshin V.V., Pryalov S.N. (2005) Fundamentals of Numerical Modeling trunk pipelines. Moscow, Dom Knigi
20. Safarov I.I., Teshayev M. Kh, Nuriddinov B. Z., Boltayev Z. I. (2017) Of Own and Forced Vibrations of Dissipative Inhomogeneous Mechanical Systems. Applied Mathematics,8: 1001-1015.
<http://www.scirp.org/journal/am>

21. Safarov, I.I., Akhmedov, M.Sh. and Boltaev, Z.I. (2015) Setting the Linear Oscillations of Structural Heterogeneity. Viscoelastic Lamellar Systems with Point Relations. Applied Mathematics. <https://doi.org/10.4236/am.2015.62022>
22. Mubarakov Y.N. (1987) Seismodynamics of underground structures such as shells. Tashkent, Fan
23. Mironov P.S. (1973) Explosions and seismic safety of structures. Moscow, Nedra
24. Pasechnik I.P. (1970) Characteristics of seismic waves in nuclear explosions and earthquakes. Moscow, Nauka
25. Kuzmina N.V., Romashov A.N., Rulev B.G., Kharin D.A. (1962) Seismic effect explosions for ejection in non-rocky cohesive soils. Transactions of Institute of Physics Earth Academy of Sciences of the USSR. 6: 3-72
26. Rulev B.G. (1964) Dynamic characteristics of seismic waves in underground explosions. In: Rulev B.G. Explosive business. Moscow, Nedra
27. Korchinsky I.L. (1971) Earthquake-resistant building construction. Moscow, Higher school
28. Mosinets V.N., Savelyev Yu.Ya. (1968) Features of the distribution of seismic waves in the field of mining. Izv. AS Kirg. SSR. 2: 8-12
29. Safonov L.V., Kuznetsov G.V. (1967) Seismic effect of borehole explosion charges. Moscow, Nauka
30. Mentuykov V.P., Silin V.S., Chekmarev V.P., Little Yu.A. (1972) Seismic explosion effect on underground pipelines. J Construction pipelines. 6: 16-18
31. Broad G. (1975) Calculations explosive on a computer. Moscow, Mir
32. Godunov S.K., Zabrodin A.V., Prokopov G.P. (1961) Difference scheme for two-dimensional non-stationary problems of gas dynamics and calculation of the flow around the departed shock wave. ZhVM and MF. 1, 6: 1020-1050.
33. Safarov I.I., Boltaev Z.I., Akhmedov M.Sh. (2015) The effect of harmonic waves on cylindrical layers with a liquid. Structural mechanics and structural analysis. 1: 74-80.
34. Safarov I.I., Teshayev M.Kh., Boltaev Z.I. (2015) On the influence of the proximity of the source of dilatation waves on the dynamic stresses of a cylinder with a liquid. Bulletin of Perm University. Mathematics, Mechanics, Computer science. Perm., 4 (31): 58-66
35. Safarov I.I., Umarov A.O., Esanov N.K. (2014) Fluctuations of buried cylindrical pipes isolated by soft soil. Materials of the X International Conference on Nonequilibrium Processes in Nozzles and Jets. Moscow, May 25-31., pp. 424-426.

36. Muhsin Khudoyberdiyevich Teshae, Ismoil Ibrohimovich Safarov, Nasriddin Urinovich Kuldashov, Tulkin Razzoqovich Ruziev, Matlab Rahmatovich Ishmamatov. On the Distribution of Free Waves on the Surface of a Viscoelastic Cylindrical Cavity. Journal of Vibration Engineering & Technologies. <https://doi.org/10.1007/s42417-019-00160-x>

37. M.Kh. Teshae, I. I. Safarov, M. Mirsaidov. (2019) Oscillations of multilayer viscoelastic composite toroidal pipes. Journal of the Serbian Society for Computational Mechanics. 13,2: 105-116.